Published in final edited form as:
Biol Psychiatry. 2011 May 15; 69(10): 989–996. doi:10.1016/j.biopsych.2010.11.021.

Abnormalities of Neuronal Oscillations and Temporal Integration to Low and High Frequency Auditory Stimulation in Schizophrenia

Jordan P. Hamm[1], **Casey S. Gilmore**[2], **Natalie A.M. Picchetti**[1], **Scott R. Sponheim**[3,4,2], and **Brett A. Clementz**[1,*]

[1]Departments of Psychology and Neuroscience BioImaging Research Center University of Georgia

[2]Department of Psychology University of Minnesota

[3]Minneapolis VA Healthcare System

[4]Department of Psychiatry, University of Minnesota

Abstract

Background—Electro- and magneto-encephalography (E/MEG) studies indicate among schizophrenia patients (SZ) abnormal, often reduced, entrained (steady-state; aSSR) and transient (N100/M100) neural responses to auditory stimuli. We complement this literature by focusing analyses on auditory cortices, assessing a wide range of stimulation frequencies with long driving periods, and evaluating relationships between aSSR and M100 reductions in SZ.

Method—Seventeen SZ and 17 healthy subjects (H) participated. Stimuli were 1500ms binaural broadband noise sequences modulated at 5, 20, 40, 80 or 160-Hz. MEG data were collected and co-registered with structural magnetic resonance images. aSSRs and M100s projected into brain space were analyzed as a function of hemisphere, stimulus density, and time.

Results—aSSR: At low (5-Hz) and high (80-Hz) modulation frequencies, SZ displayed weaker entrainment bilaterally. To 40-Hz stimuli, SZ showed weaker entrainment only in right auditory cortex. M100: While responses for H increased linearly with stimulus density, this effect was weaker or absent in SZ. Relationship: A principal components analysis of SZ deficits identified low (5-Hz entrainment and M100) and high (40–80-Hz entrainment) frequency components. Discriminant analysis indicated that the low frequency component uniquely differentiated SZ from H. The high frequency component correlated with negative symptoms among SZ.

Conclusions—SZ auditory cortices were unable to (i) generate healthy levels of theta- and high gamma-band (80Hz) entrainment (aSSR) and (ii) augment transient responses (M100s) to rapidly presented auditory information (an index of temporal integration). Only the latter was most apparent in left hemisphere, and may reflect a prominent neurophysiological deficit in schizophrenia.

*Corresponding Author Psychology Department, Psychology Building, Baldwin Street, University of Georgia, Athens GA 30602, clementz@uga.edu.

Keywords

Schizophrenia; Magnetoencephalography; auditory steady-state; M100; gamma; theta

Electro- and magneto-encephalography (E/MEG) studies indicate that schizophrenia patients (SZ) have abnormalities of the auditory entrained steady-state (aSSR) and evoked N100/M100 responses (1, 2). The aSSR reflects a response to auditory stimuli repeated at a constant and rapid rate (e.g., 20-Hz is a stimulus every 50 ms; 40-Hz a stimulus every 25 ms). The aSSR cortical generators lie mainly in Heschl's gyrus (3, 4, 5) and are believed to arise from interactions between thalamo-cortical glutamatergic stimulation and intrinsic local network oscillations (3,6) driven by GABA-ergic modulation of pyramidal cells (7–10). The auditory N100/M100 occurs in relation to transient and abrupt stimuli separated by relatively large inter-stimulus intervals (e.g., greater than 1000 ms), and is generated largely in subgranular layers of planum temporale (11–14). Both deviations among SZ are hypothesized to be caused by deficient N-Methyl-D-aspartate (NMDA)-mediated transmission in thalamo-cortical and cortical-cortical projections (2, 15, 16) and/or altered modulation of pyramidal cells by GABA-ergic interneurons in local cortical networks (17).

Brain responses at the steady-state stimulation frequency probe the integrity of auditory thalamo-cortical inputs, and ability of the auditory system to maintain spatially coherent, phase-locked entrainment to those stimuli (18). SZ show reduced 40-Hz (8 of 10 studies; 19–28) but not 20-Hz (19, 21–23, 25, 26, 28) aSSRs. Brenner et al (19) examined aSSRs at frequencies from 11 to 82-Hz, and reported reduction across frequencies among SZ, but individual stimulation frequency effects and their temporal nature were not specified.

N100/M100 amplitudes are normally enhanced by increasing information `density' in the first 50 ms after stimulus onset (29). For example, as the number of stimuli in the first 50 ms increased from 1 (10-Hz stimulation rate) to 5 (80-Hz stimulation rate), Gilmore, Clementz, and Buckley (30) found that healthy subjects, but not SZ, increased N1/P2 amplitudes. This indicated that SZ auditory processing problems are worsened when requiring rapid integration of auditory information, which may depend on intact thalamo-cortical NMDA-mediated excitatory drive (9).

The present study used MEG to examine the aSSR and M100 across a range of stimulation frequencies, which allowed for evaluation of the temporal stability and rapid summation of auditory processing among SZ. Use of MEG and source localization models based on individual head geometries allowed for specific evaluation of auditory cortical processing and hemispheric laterality among SZ (31). Four issues were addressed: First, do SZ display deficient neural entrainment at frequencies higher than 40-Hz? The answer will help clarify whether SZ aSSR reductions are due to general abnormalities of gamma range neural oscillators (deficient GABAergic coordination of pyramidal cells; 10) or are specific to 40-Hz aSSR resonance (18). Second, can SZ maintain an aSSR over time (1500 ms)? Most studies use 500 ms stimulation periods (2; 23 used 1000 ms) even though the aSSR requires at least 240 ms to develop (3). Third, will high stimulus densities accentuate differences between SZ and healthy subjects on auditory cortical M100 responses (30)? This effect has not been replicated, and it is unknown if M100 amplitude reductions among SZ are associated with temporal summation in auditory cortex, theoretically dependent on NMDA-mediated signaling (9). Fourth, the relationship between aSSR and M100 deficits among SZ is unknown, so it is uncertain if they are part of a common neuropathology.

To address the first 2 issues, evoked amplitudes in brain space and inter-trial phase coherence (ITC) at each driving frequency (aSSRs) were quantified to determine whether

magnitude and/or temporal consistency of neural entrainment accounts for group differences. To address the third issue, auditory neural responses evoked by stimulus onset (M100) were analyzed as a function of stimulus modulation frequency. Linear increases in amplitudes due to increasing stimulus density were then compared between groups. To characterize the relationship between aSSR and M100 deficits in SZ, principal component analysis was computed using measures that differentiated groups to establish which measures covary and determine whether one or multiple subsets of auditory cortical deficits differentiate SZ from healthy subjects.

Methods

Subjects

Eighteen SZ (Mean age=40.7 years, SD=9.6; 2 females; all right-handed) and 18 healthy (H) subjects (Mean age = 39.7 years, SD=11.4; 5 females; one left-handed) participated (see Table 1). Data were collected at the Brain Sciences Center of the Minneapolis VA Medical Center. SZ were recruited from VA outpatient clinics, community support programs, and a county mental health clinic. Healthy subjects were recruited through community announcements and were absent of Axis I psychopathology (save one subject with dysthymia). Subjects were absent of current alcohol or drug abuse, past drug dependence, current or past central nervous system disease or condition, history of head trauma, and possibly confounding treatments (e.g. electroconvulsive therapy). A trained doctoral-level clinical psychologist determined presence of SZ specifically and confirmed the absence of disallowed conditions through administering the Diagnostic Interview for Genetic Studies (DIGS; 32). Scales for the Assessment of Negative (SANS, 33) and Positive Symptoms (SAPS, 34), and Brief Psychiatric Rating Scale (BPRS, 35) quantified severity and extent of symptomology. Fifteen SZ were receiving clinical doses of atypical antipsychotics; one was receiving a conventional antipsychotic (haloperidol). The remaining two SZ were not receiving antipsychotic medication at the time of testing (see Supplemental Methods for a list of medications). Subjects provided written informed consent. This study was approved by University of Georgia, Minneapolis VA Medical Center, and University of Minnesota Institutional Review Boards.

Stimuli and procedure

Steady-state stimuli consisted of 1500 ms broadband noise bursts (bandpass filtered 500–4000 Hz; 18) amplitude modulated (100% depth) at 5, 20, 40, 80, or 160-Hz. Noise bursts were presented binaurally through plastic tubes at 76-dB SPL. Each frequency of stimulation was presented in a separate block, with each block consisting of 100 trials with an average 3000 ms stimulus-onset asynchrony (range 2700–3300 ms). To control attention, unmodulated noise bursts (also 76-dB) lasting 1500 ms were presented on 10% of trials, to which subjects were to respond with a button press. Unmodulated bursts were evaluated for correct detections.

Data acquisition

Data were collected using a 248-channel axial gradiometer MEG system (Magnes 3600 WH, 4D-Neuroimaging, San Diego, CA, USA). Digitization of scalp and fiducial points was accomplished with a Polhemus Fastrak 3-D digitizer (Polhemus, Colchester, VT, USA). Eye movements and eyeblinks were monitored using three electrodes placed around the right eye. Data were acquired at 1,017.25 Hz and analogue-filtered at 0.1–400 Hz.

MEG data screening

MEG data were screened and segmented around stimulus triggers using BESA 5.2.2 (MEGIS Software, Grafelfing, Germany). Data were inspected for bad channels and trials containing blink or cardiac artifacts. When present, artifacts were removed using Independent Components Analysis (EEGLAB 6.0; 36). Bad channels were interpolated (no more than 5% of channels for any subject) using spherical spline interpolation. Trials containing activity greater than 3000 femtoTesla were eliminated. One SZ was dropped due to low quality data; one H was dropped because greater than 40% of trials were eliminated (an outlier on number of usable trials). The number of useable trials did not differ between groups (Table 1). Data were sub-sampled to 1000 Hz and digitally bandpass filtered from 1–200 Hz (zero-phase; rolloff: 6 dB/octave highpass, 48 dB/octave lowpass). Trials consisted of 3000 ms epochs, beginning 500 ms before stimulus onset.

MRI acquisition and co-registration

Magnetic Resonance Images (MRIs) were obtained using a 3D MPRAGE protocol (TR=11.4 sec, TE=4.4 sec, flip angle 10 deg, FOV=256 mm, 1 mm isotropic resolution) across a 128 mm axial slab. Using Brain Voyager V2.0 (Brain Innovation, The Netherlands), MR data were aligned along the AC/PC line. Scalps and cortical surfaces were manually segmented based on voxel intensity. Fiducial points (nasion, left and right pre-auricular points) were identified for coregistration with the MEG data. These procedures resulted in individual head models used for subsequent analyses. One subject (H) did not have MRIs collected, and another subject's (SZ) MR data were incomplete. For these subjects, standard MNI head models were used.

Data analyses

The presence of aSSRs at all frequencies was examined for each stimulus type (see Supplemental Methods). All driving frequencies except 160-Hz resulted in above-baseline ITC (Figure S2 in the Supplement) and passed a *Circ-T* test for cross trial oscillatory consistency (37), with all passing aSSRs present in all subjects at $p<.01$. ECOG studies indicate that polyphasic summation across neighboring neurons low-pass filters high frequency activity recorded outside the head (38); therefore, cortical aSSRs >100-Hz are difficult to detect with MEG (18). [The 160-Hz stimulation condition, however, was included to study temporal summation effects on the M100.] The only non-driving frequency with an above baseline aSSR was the 40-Hz harmonic to 20-Hz stimulation.

The frequency characteristics of responses with significant oscillatory activity in the above analyses were assessed by calculating inter-trial phase coherence (ITC; phase consistency of oscillations across trials; 39, 40) for each time point (−500 to 2500 ms), subject, condition, and MEG sensor (see Supplemental Methods) at 2.5-Hz frequency resolution. Sensors capturing the aSSR (Figure 1) and M100 (Figure 2) were used for group comparisons.

Averaged epochs of MEG data were co-registered with individual head models so fields measured at the sensors could be analyzed in source space. For the M100, peak latencies between 75 and 150 ms were identified, separately for each hemisphere, based on projection of the magnetic field across the modeled scalp surface (Figure S1 in the Supplement) and global field power. A manual procedure was used to ensure that a peak with the correct orientation was used (superior-inferior dipolar configuration). Source analysis of the aSSR required additional processing to isolate evoked responses. One approach (e.g. 20) is to use bandpass filtering to isolate activity at a given frequency of interest. Yvert et al (11), however, showed that high pass filters above 3-Hz may spatially distort auditory responses. To avoid such possible distortion, high-pass filters were kept at 1 Hz, and magnetic data at the 5, 20, 40, and 80-Hz frequencies were isolated with the combined use of low-pass filters

(8, 35, 55, and 100 Hz, respectively) and a moving window averaging procedure (41): (i) 3000 ms epochs averaged over trials for each subject and frequency were segmented into 6 consecutive 500 ms bins; (ii) For each bin, a one-cycle window was moved in steps of one cycle and summed at each step to create an average waveform representing one cycle of the oscillatory response within the associated bin. This bolstered the signal only for activity at the frequency of interest; (iii) This procedure was repeated for all channels within an epoch and resulted in six separate evoked response periods during auditory driving (500 ms pre-stimulus, 0–500, 500–1000, and 1000–1500 ms during stimulation, and two 500 ms bins following stimulus offset).

Distributed cortical source generators of the aSSR and M100 were modeled using L2 minimum norm with spatio-temporal depth weighting in BESA (42) for each subject and were spatially converted to a standard MNI brain for group comparisons using a nearest neighbor approach. The aSSR and M100 activities in left and right auditory cortices were quantified by calculating the average of the peak activation and its 6 nearest neighbors.

Statistical analysis

For ITC, independent-samples t-tests were calculated for each location in time by frequency space (see Figures 1 and 2). Based on Monte Carlo simulations (43), to maintain the familywise alpha at $p<.010$ the number of adjacent points in the time-frequency plots that needed to have a p-value <.025 was 8 for the driving frequency and 6 for the M100 analyses. The aSSR amplitudes were analyzed in two steps: (i) a Group Membership (SZ, H) by Hemisphere (Left, Right) by Rate of Stimulation (5, 20, 40, 80-Hz) by Time (500 ms pre-stimulus; first and second 500 ms bins following stimulus offset) mixed-model ANOVA for evaluating baseline offsets; and (ii) a Group Membership by Hemisphere by Rate of Stimulation by Time (first, second, and third 500 ms bins during steady-state stimulation) mixed-model ANOVA to evaluate neural responses to auditory driving. The 40-Hz harmonic was analyzed separately from the driving frequencies.

M100 latencies were analyzed using a Group Membership by Hemisphere by Rate of Stimulation (5, 20, 40, 80, 160-Hz) mixed-model ANOVA. M100 amplitude increases linearly with stimulus density (29, 30). Thus, M100 source current strengths (the dependent variable) were regressed on stimulus density (the independent variable; which was coded as $\log_2$ of the number of stimulus repetitions during the first 50 ms after trial onset: 5-Hz=0, 20-Hz=1, 40-Hz=2, 80-Hz=3, 160-Hz=4). This approach yielded slopes and intercepts for each subject. These values were separately subjected to Group Membership by Hemisphere AVOVAs. For all ANOVAs, Greenhouse-Geisser degrees of freedom correction was used when sphericity was violated (Mauchly's test of Sphericity; 44).

Results

Behavior

Percent correct responses to the unmodulated noise bursts did not differ between H (Mean=99.0%, SD=1.5) and SZ (Mean=97.3%, SD=4.1), indicating that the groups were equally attentive to the stimuli.

Inter-Trial Coherence of Auditory Neural Response

aSSR (Figure 1)—There were no between-group hemispheric differences, so these results are presented collapsing over this factor. The groups differed on ITC for the 5 and 80-Hz driving frequencies, with SZ having lower ITC; the groups did not differ on ITC to the 20 and 40-Hz driving frequencies or the 40-Hz harmonic. These effects were stable throughout the steady-state period.

M100 (Figure 2)—Across stimulation frequencies, ITC effects were the same so these results are presented collapsing over this factor. SZ had lower ITC in the delta and theta frequency ranges at the time of the M100 (from 50 to 150 ms post-stimulus) in left but not right hemisphere. SZ also had attenuated ITC in right hemisphere during a later interval (200–600 ms post-stimulus), but this difference was more dramatic (peak effect size d=2.28 vs d=1.67) and exhibited a larger spectral/temporal extent in left hemisphere.

Amplitudes of Neural Activity in Auditory Cortex

aSSR (Figure 3)—Oscillatory amplitudes at the driving frequencies in the pre- and post-stimulus intervals did not differentiate groups, indicating that SZ and H did not differ on baseline oscillatory power. For the analysis of aSSR stimulation periods (0–1500 ms), there was a significant main effect of Group, $F(1,32)=5.05$, $p<.05$, and a significant Hemisphere by Frequency by Group interaction, $F(3,96)=3.83$, $p<.05$. There were no other significant effects involving Group. SZ had lower aSSR amplitudes than H across driving frequencies. To clarify the interaction, ANOVAs were repeated for each level of the driving frequency. At 5-Hz, there was only a main effect of Group, $F(1,32)=5.124$, $p<.05$, with SZ having lower amplitude responses. At 20-Hz, there were no significant effects involving Group. At 40-Hz, there was only a Hemisphere by Group interaction, $F(1,32)=4.95$, $p<.05$, with SZ having lower response amplitudes specifically in right hemisphere. At 80-Hz, there was only a main effect of Group, $F(1,32)=4.69$, $p<.05$, with SZ having lower amplitude responses. For the 40-Hz harmonic, there was a significant Group by Time interaction, $F(2,64)=3.96$, $p<.05$, with H having stronger evoked amplitudes bilaterally during the last 1000 ms of stimulation.

M100 (Figure 4)—On M100 latencies, SZ (M=111.4 ms, SE=4.1) and H (M=105.3 ms, SE=3.1) did not differ significantly. Regression of M100 amplitude on stimulus density was conducted separately by hemisphere. For left hemisphere, M100 amplitude in nanoamperes (y) as a function of stimulus frequency (x) was modeled for SZ as $y = 0.8(SE=0.3)x + 10.3(SE=1.9)$ and for H as $y = 2.1(SE=0.6)x + 17.2(SE=2.3)$. For right hemisphere, M100 amplitude was modeled for SZ as $y = 0.2(SE=0.4)x + 11.3(SE=1.6)$ and for H as $y = 1.1(SE=0.5)x + 12.3(SE=1.8)$. For the slope term, there were main effects of Hemisphere, $F(1,32)=4.92$, $p<.05$, and Group, $F(1,32)=4.70$, $p<.05$. M100 amplitudes in left hemisphere increased more dramatically with respect to stimulus density than those in right hemisphere, but, compared to H, SZ M100s were less sensitive to changes in stimulus density. This resulted in lower overall M100 amplitude in SZ (M=12.1 nanoamperes, SE=1.6) compared to H (M=21.8 nanoamperes, SE=2.8). For the intercept term, there were no significant effects.

Principal Components and Discriminant Analysis

To explore relationships between aSSR and M100 deficits, principal components analysis (PCA with Kaiser normalization and PROMAX rotation; 45) was used to summarize covariation within-subjects using variables that differentiated groups: M100 slopes, left hemisphere M100 ITC (averaged across stimulation frequencies), right hemisphere aSSR 40-Hz evoked amplitude, 40-Hz harmonic aSSR evoked amplitude during the last 1000 ms of stimulation, and 5 and 80-Hz aSSR evoked amplitudes and ITC. These 8 variables yielded a variable to item ratio of close to 5:1 (46). To determine the number of components to retain from the PCA, a criterion more rigorous than Kaiser's (47) “eigenvalue>1” rule was adopted based on Lautenschlager (48; Supplemental Methods), resulting in retention of 2 factors (see Table 2). Bartlett factor scores were calculated for all participants for each factor and compared between-groups using independent samples t-tests (two-tailed, df=32). The first factor (low-frequency/transient-evoked activity) significantly differentiated groups, with SZ (M=−0.48, SE=.14) having lower scores than H (M=0.48, SE=.28). The second

factor (gamma activity) also significantly differentiated groups, with SZ (M=−0.42, SE=.15) having lower scores than H (M=0.42, SE=.29). The discriminating power of each factor was tested by assessing whether addition of factor scores to a discriminant analysis significantly incremented group discrimination variance after inclusion of the other factor. The first factor significant incremented group discrimination variance beyond the second factor, $F(1,31)=6.09$, $p=.019$, whereas the second factor did not increment group discrimination variance beyond the first factor, $F(1,31)=3.40$, $p>.05$.

Correlations with symptom ratings

Symptom ratings were correlated with brain activity measures that differentiated the two groups as summarized by the two factor scores. The only significant effect was an inverse correlation of negative symptoms (SANS) with factor 2 (gamma aSSR) at r=−.49 (p=.039), which was primarily due to a stronger negative correlation of negative symptoms with 80-Hz aSSR amplitude at r=−.55, p=.025 (Figure S3 in the Supplement).

Discussion

Despite being attentive to the ongoing task, SZ displayed abnormal oscillatory and transient neural responses in auditory cortex. Most notably, SZ showed aSSR deficits in the high gamma range (80-Hz); evoked amplitude and ITC were reduced bilaterally. To 40-Hz steady-state stimuli, SZ amplitude reductions were specific to right auditory cortex within the context of normal ITC. Consistent with previous reports (22), SZ showed normal beta range aSSRs (20-Hz), but reduced gamma range entrainment bilaterally at the harmonic (40-Hz). Similar to the findings in response to 40-Hz stimulation, the 40-Hz harmonic reduction involved evoked amplitude but not ITC. To theta range stimuli (5-Hz), SZ had decreased aSSRs bilaterally on both evoked amplitudes and ITC. SZ also had lower theta range (2.5–7.5 Hz) ITC to stimuli onsets and M100 amplitudes, effects that were most dramatic in left hemisphere. M100 effects were exacerbated at higher stimulus densities, with SZ failing to benefit from increased information content. This result replicates and localizes Gilmore et al's (30) finding that SZ N100 responses are most reduced at high stimulus densities.

Evoked field amplitudes are a combination of stimulus-locked oscillatory phase alignment (ITC) and amplitude augmentation to single stimuli (39, 49). Thus, the current findings indicate that SZ auditory cortical entrainment abnormalities to 5 and 80-Hz stimuli involve deficient temporal consistency of neural responses across trials (ITC) and reduced recruitment/coherence in local auditory cortical networks (amplitude). Entrainment abnormalities at 40-Hz, however, primarily reflect lower amplitude augmentation (49). Whether this discrepancy indicates separate neurophysiological deficits or a difference in the effect size of the same deficiency is unclear and requires future investigation.

One study of the aSSR in SZ included theta range stimuli (21) and one study included stimuli above 50-Hz (19), but those reports described aSSR reductions in SZ across a broad stimulation range (>8 different stimuli) and did not specifically examine aSSR effects at individual frequencies with respect to lateralized auditory cortical sources. The current findings, therefore, provide a unique glimpse at theta (5-Hz) and high gamma range (80-Hz) auditory entrainment abnormalities in bilateral auditory cortices among SZ. Of 10 studies examining 40-Hz aSSRs in SZ (19–28), 8 found reductions consistent with the current results; the laterality of 40-Hz aSSR reductions reported here (right hemisphere) differ from 3 reports (2 MEG studies) of left hemisphere reductions (20, 24, 25). Like the current study, 7 investigations of 20-Hz aSSRs reported normal entrainment among SZ (19, 21–23, 25–26, 28) with the exception of one study (25) reporting augmented 20-Hz responses. The deficit of entrained 40-Hz activity to 20-Hz stimulation (harmonic) has been reported in 2 of these

studies (22, 25); the current results replicate this effect and show it is worse after prolonged stimulation.

Of note, the current study required subjects attend to, rather than either passively listen (e.g 19–20, 22–28) or ignore (21), the stimuli. Gamma-range (40-Hz), but not 20-Hz, responses are sensitive to attentional modulation (50) which may explain some discrepancies in the literature. The current study also used amplitude modulated white noise as opposed to click (22–28) or tone (21, 22) stimuli, which might excite an extended region of auditory cortex (18). Combined with longer stimulus durations, these differences may have driven SZ cortical neural ensembles to oscillate at healthy levels (at least at low gamma frequencies). Future work will be needed under varying stimulus presentation conditions to more completely understand these discrepancies.

GABAergic interneurons containing parvalbumin (PV) modulate both theta (51) and gamma range (52) pyramidal cell activity. Expression of PV mRNA in GABAergic interneurons is decreased in SZ prefrontal, anterior cingulate, visual, and motor cortices (53). The theta- and gamma-range entrainment abnormalities reported here suggest that PV containing interneurons are also disrupted in SZ auditory cortices, and may constitute a significant functional consequence of this neuropathology in mesoscopic neural networks.

PV containing GABAergic interneurons that modulate theta and gamma range oscillations receive excitatory inputs from NMDA receptors (54), hypofunction of which have been associated with SZ (55). Neural response amplitude augmentation to temporally dense stimuli (increasing M100 to higher frequency stimuli) relies on temporal integration in superior temporal lobe neural assemblies (29), and such temporal summation in thalamo-cortical and cortico-cortical circuits may depend on NMDA-receptor mediated glutamatergic transmission (9). Chronic NMDA-antagonism (as opposed to acute administration of NMDA antagonists) produces alterations in GABAergic interneurons (56, 57) similar to those seen in SZ, although effects on gamma and theta range aSSRs or M100 temporal summation are not specifically known.

The aSSR reductions to 40-Hz steady state stimuli were right lateralized and involved lower amplitude, but not lower ITC, suggesting a deficit in the magnitude, rather than the temporal consistency, of stimulus-evoked activity. The 40-Hz aSSR was relatively enhanced in right hemisphere among healthy subjects. Since right auditory cortex plays a role in frequency/pitch discrimination (58), reductions in SZ may reflect the absence of appropriate task-related neural facilitation. For instance, cholinergic muscarinic receptors modulate gamma generating interneuron assemblies (10) and are reduced by about 75% among SZ (59).

A PCA segregated covariance among aSSR and M100 deficits into low (5-Hz entrainment and M100) and high frequency factors (40 and 80-Hz entrainment). Although both factors differentiated groups, discriminant analyses revealed that only the low frequency factor added significantly to group discrimination, but the high frequency factor correlated with negative symptoms among SZ. Perhaps M100 and theta band entrainment abnormalities are ubiquitous among SZ, with gamma range abnormalities characterizing patients with more pronounced negative symptoms. Of course, the effects of medication on aSSR deficits in SZ are uncertain, so medication effects cannot be eliminated as an explanation for these effects. Of importance, however, gamma range reductions during a visual working memory task are present in unmedicated SZ (60), which also holds true for auditory N100 reductions (1).

The two PCA factors could be related to a single abnormality in SZ. The ability of secondary auditory cortex to generate M100 (14) and temporally integrate auditory information at higher stimulus densities may depend on the ability of primary auditory cortex to establish, and relay, coherent high frequency oscillations (as measured by gamma

aSSR, 4). N/M100 reductions in SZ may reflect disruptions in temporal summation in local auditory cortical circuitry. The consequences of such a functional disconnection may be consistent with neuroanatomical studies suggesting that feed-forward pathways and/or synaptic connectivity between primary and secondary auditory cortex are diminished in SZ (61,62), and comprise a promising avenue for research into the neurobiological basis for electrophysiological correlates of auditory processing abnormalities in schizophrenia.

Supplementary Material

Refer to Web version on PubMed Central for supplementary material.

Acknowledgments

The authors are grateful to John J. Stanwyck, Amy L. Silberschmidt, and Arthur Leuthold Ph.D. for their assistance with data collection and management, as well as the support of Brain Sciences Center personnel at the Minneapolis VA Medical Center. This work was supported by grants from the United States Public Health Service (MH57886, R24MH069675).

References

1. Rosburg T, Boutros NN, Ford JM. Reduced auditory evoked potential component N100 in schizophrenia--a critical review. Psychiatry Res. 2008; 161(3):259–74. [PubMed: 18926573]
2. Brenner CA, Krishnan GP, Vohs JL, Ahn WY, Hetrick WP, Morzorati SL, O'Donnell BF. Steady state responses: electrophysiological assessment of sensory function in schizophrenia. Schizophrenia Bulletin. 2009; 35:1065–77. [PubMed: 19726534]
3. Ross B, Picton TW, Pantev C. Temporal integration in the human auditory cortex as represented by the development of the steady-state magnetic field. Hearing Research. 2002; 165:68–84. [PubMed: 12031517]
4. Gutschalk A, Mase R, Roth R, Ille N, Rupp A, Hähnel S, Picton TW, Scherg M. Deconvolution of 40 Hz steady-state fields reveals two overlapping source activities of the human auditory cortex. Clinical Neurophysiology. 1999; 110:856–68. [PubMed: 10400199]
5. Hari R, Hamalainen M, Joutsiniemi SL. Neuromagnetic steady-state responses to auditory stimuli. Journal Acoustical Society of America. 1989; 86:1033–9.
6. Santarelli R, Conti G. Generation of auditory steady-state responses: linearity assessment. Scand Audiol Suppl. 1999; 51:23–32. [PubMed: 10803911]
7. Whittington MA, Traub RD, Jefferys JGR. Synchronized oscillations in interneuron networks driven by metabotropic glutamate receptor activation. Nature. 1995; 373:613–5.
8. Bacci A, Hueuenard J. Enhancement of Spike-Timing Precision by Autaptic Transmission in Neocortical Inhibitory Interneurons. Neuron. 2006; 49:119–30. [PubMed: 16387644]
9. Gonzalez-Burgos G, Lewis DA. GABA neurons and the mechanisms of network oscillations: implications for understanding cortical dysfunction in schizophrenia. Schizophr Bulletin. 2008; 34:944–61.
10. Bartos M, Vida I, Jonas P. Synaptic mechanisms of synchronized gamma oscillations in inhibitory interneuron networks. Nat Rev Neurosci. 2007; 8:45–56. [PubMed: 17180162]
11. Yvert B, Fischer C, Bertrand O, Pernier J. Localization of human supratemporal auditory areas from intracerebral auditory evoked potentials using distributed source models. Neuroimage. 2005; 28:140–53. [PubMed: 16039144]
12. Javitt DC. Intracortical mechanisms of mismatch negativity dysfunction in schizophrenia. Audiol Neurootol. 2000; 5:207–15. [PubMed: 10859415]
13. Barth DS, Di S. The functional anatomy of middle latency auditory evoked potentials. Brain Research. 1991; 565:109–15. [PubMed: 1773348]
14. Naatanen R, Picton T. The N1 wave of the human electric and magnetic response to sound: a review and an analysis of the component structure. Psychophysiology. 1987; 24:375–425. [PubMed: 3615753]

15. Ehlers CL, Kaneko WM, Wall TL, Chaplin RI. Effects of dizocilpine (MK-801) and ethanol on the EEG and event-related potentials (ERPS) in rats. Psychiatry Res. 1992; 161(3):259–74.

16. Ehrlichman RS, Gandal MJ, Maxwell CR, Lazarewicz MT, Finkel LH, Contreras D, Turetsky BI, Siegel SJ. N-methyl-D-aspartic acid receptor antagonist-induced frequency oscillations in mice recreate pattern of electrophysiological deficits in schizophrenia. Neuroscience. 2009; 158:705–12. [PubMed: 19015010]

17. Uhlhaas PJ, Singer W. Abnormal neural oscillations and synchrony in schizophrenia. Nature Reviews Neuroscience. 2010; 11:100–13.

18. Picton TW, John MS, Dimitrijevic A, Purcell D. Human auditory steady-state responses. International Journal of Audiology. 2003; 44:177–219. [PubMed: 12790346]

19. Brenner CA, Sporns O, Lysaker PH, O'Donnell BF. EEG synchronization to modulated auditory tones in schizophrenia, schizoaffective disorder, and schizotypal personality disorder. American Journal of Psychiatry. 2003; 160:2238–40. [PubMed: 14638599]

20. Teale P, Collins D, Maharajh K, Rojas DC, Kronberg E, Reite M. Cortical source estimates of gamma band amplitude and phase are different in schizophrenia. Neuroimage. 2008; 42:1481–89. [PubMed: 18634887]

21. Krishnan GP, Hetrick WP, Brenner CA, Shekhar A, Steffens AN, O'Donnell BF. Steady state and induced auditory gamma deficits in schizophrenia. Neuroimage. 2009; 47:1711–1719. [PubMed: 19371786]

22. Spencer KM, Salisbury DF, Shenton ME, McCarley RW. Gamma-band auditory steady-state responses are impaired in first episode psychosis. Biol Psychiatry. 2008; 64:369–375. [PubMed: 18400208]

23. Light GA, Hsu JL, Hsieh MH, et al. Gammaband oscillations reveal neural network cortical coherence dysfunction in schizophrenia patients. Biol Psychiatry. 2006; 60:1231–1240. [PubMed: 16893524]

24. pencer KM, Niznikiewicz MA, Nestor PG, Shenton ME, McCarley RW. Left auditory cortex gamma synchronization and auditory hallucination symptoms in schizophrenia. BMC Neurosci. 2009; 20:10–85.

25. Vierling-Claassen D, Siekmeier P, Stufflebeam S, Kopell N. Modeling GABA alterations in schizophrenia: a link between impaired inhibition and altered gamma and beta range auditory entrainment. J Neurophysiol. 2008; 99:2656–2671. [PubMed: 18287555]

26. Kwon JS, O'Donnell BF, Wallenstein GV, et al. Gamma frequency range abnormalities to auditory stimulation in schizophrenia. Arch Gen Psychiatry. 1999; 56:1001–1005. [PubMed: 10565499]

27. Teale P, Carlson J, Rojas D, Reite M. Reduced laterality of the source locations for generators of the auditory steadystate field in schizophrenia. Biol Psychiatry. 2003; 54:1149–1153. [PubMed: 14643081]

28. Hong LE, Summerfelt A, McMahon R, et al. Evoked gamma band synchronization and the liability for schizophrenia. Schizophr Res. 2004; 70:293–302. [PubMed: 15329305]

29. Forss N, Makela JP, McEvoy L, Hari R. Temporal integration and oscillatory responses of the human auditory cortex revealed by evoked magnetic fields to click trains. Hearing Research. 1993; 68:89–96. [PubMed: 8376218]

30. Gilmore CS, Clementz BA, Buckley PF. Rate of stimulation affects schizophrenia-normal differences on the N1 auditory-evoked potential. Neuroreport. 2004; 18:2713–7. [PubMed: 15597040]

31. Lu BY, Edgar JC, Jones AP, Smith AK, Huang MX, Miller GA, Canive JM. Improved test-retest reliability of 50-ms paired-click auditory gating using magnetoencephalography source modeling. Psychophysiology. 2007; 44:86–90. [PubMed: 17241143]

32. Nurnberger JI Jr, Blehar MC, Kaufmann CA, York-Cooler C, Simpson SG, Harkavy-Friedman J, Severe JB, Malaspina D, Reich T. Diagnostic interview for genetic studies. Rationale, unique features, and training. NIMH Genetics Initiative. Arch Gen Psychiatry. 1994; 51:849–59. [PubMed: 7944874]

33. Andreasen, NC. Scale for the Assessment of Negative Symptoms (SANS). University of Iowa; Iowa City: 1981.

34. Andreasen, NC. Scale for the Assessment of Positive Symptoms (SAPS). University of Iowa; Iowa City: 1983.
35. Overall JE, Gorham DR. The brief psychiatric rating scale. Psychological Reports. 1962; 10:799–812.
36. Delorme A, Makeig S. EEGLAB: an open source toolbox for analysis of single-trial EEG dynamics. J Neurosci Methods. 2004; 134:9–21. [PubMed: 15102499]
37. Victor JD, Mast J. A new statistic for steady-state evoked potentials. Electroencephalogr Clin Neurophysiol. 1991; 78:378–38. [PubMed: 1711456]
38. Pfurtscheller G, Cooper R. Frequency dependence of the transmission of the EEG from cortex to scalp. Electroencephalography Clinical Neurophysiology. 1975; 38:93–6.
39. Moratti S, Clementz BA, Gao Y, Ortiz T, Keil A. Neural mechanisms of evoked oscillations: Stability and interaction with transient events. Human Brain Mapping. 2007; 28:1318–33. [PubMed: 17274017]
40. Hamm JP, Dyckman KA, Ethridge LE, McDowell JE, Clementz BA. Preparatory activations across a distributed cortical network determine express saccade production in humans. J. Neurosci. 2010; 30:7350–7357. [PubMed: 20505102]
41. Clementz BA, Wang J, Keil A. Normal electrocortical facilitation but abnormal target identification during visual sustained attention in schizophrenia. J Neurosci. 2009; 28:13411–13418. [PubMed: 19074014]
42. Hämäläinen MS, Ilmoniemi RJ. Interpreting magnetic fields of the brain: minimum norm estimates. Med Biol Eng Comput. 1994; 32:35–42. [PubMed: 8182960]
43. Cox LA. Reassessing benzene risks using internal doses and Monte-carlo uncertainty analysis. Environ Health Perspect. 1996; 104:1413–1429. [PubMed: 9118928]
44. Mauchly JW. Significance test for sphericity of a normal *n*-variate distribution. Annuals of Mathematical Statistics. 1940; 11:204–209.
45. Dien J. The ERP PCA Toolkit: an open source program for advanced statistical analysis of event-related potential data. J Neurosci Methods. 2010; 187:138–45. [PubMed: 20035787]
46. Gorsuch, RL. Factor Analysis. 2nd. Ed. Erlbaum; Hillsdale, NJ: 1983.
47. Kaiser HF. The application of electronic computers to factor analysis. Educational and Psychological Measurement. 1960; 20:141–51.
48. Lautenschlager GJ. A Comparison of alternatives to conducting Monte Carlo analyses for determining parallel analysis criteria. Multivariate Behavioral Research. 1989; 24:365–95.
49. Shah AS, Bressler SL, Knuth KH, Ding M, Mehta AD, Ulbert I, Schroeder CE. Neural dynamics and the fundamental mechanisms of event-related brain potentials. Cerebral Cortex. 2004; 14:476–483. [PubMed: 15054063]
50. Skosnik PD, Krishnan GP, O'Donnell BF. The effect of selective attention on the gamma-band auditory steady-state response. Neurosci Lett. 2007; 420:223–228. [PubMed: 17556098]
51. Klausberger T, Magill PJ, Márton LF, Roberts JD, Cobden PM, Buzsáki G, Somogyi P. Brain-state- and cell-type-specific firing of hippocampal interneurons in vivo. Nature. 2003; 421:844–8. [PubMed: 12594513]
52. Tukker JJ, Fuentealba P, Hartwich K, Somogyi P, Klausberger T. Cell type-specific tuning of hippocampal interneuron firing during gamma oscillations in vivo. J Neurosci. 2007; 27:8184–8189. [PubMed: 17670965]
53. Hashimoto T, Volk DW, Eggan SM, Mirnics K, Pierri JN, Sun Z, Sampson AR, Lewis DA. Gene expression deficits in a subclass of GABA neurons in the prefrontal cortex of subjects with schizophrenia. J Neurosci. 2008; 23:6315–6326. [PubMed: 12867516]
54. Kinney JW, Davis CN, Tabarean I, Conti B, Bartfai T, Behrens MM. A specific role for NR2A-containing NMDA receptors in the maintenance of parvalbumin and GAD67 immunoreactivity in cultured interneurons. J Neurosci. 2006; 26:1604–1615. [PubMed: 16452684]
55. Javitt DC. Glutamate and schizophrenia: phencyclidine, N-methyl-D-aspartate receptors, and dopamine-glutamate interactions. Int Rev Neurobiol. 2007; 78:69–108. [PubMed: 17349858]

56. Bullock WM, Bolognani F, Botta P, Valenzuela CF, Perrone-Bizzozero NI. Schizophrenia-like GABAergic gene expression deficits in cerebellar Golgi cells from rats chronically exposed to low-dose phencyclidine. Neurochem Int. 2009; 55(8):775–82. [PubMed: 19651169]
57. Braun I, Genius J, Grunze H, Bender A, Möller HJ, Rujescu D. Alterations of hippocampal and prefrontal GABAergic interneurons in an animal model of psychosis induced by NMDA receptor antagonism. Schizophr Res. 2007; 97(1–3):254–63. [PubMed: 17601703]
58. Pugh KR, Offywitz BA, Shaywitz SE, Fulbright RK, Byrd D, Skudlarski P, Shankweiler DP, Katz L, Constable RT, Fletcher J, Lacadie C, Marchione K, Gore JC. Auditory selective attention: an fMRI investigation. Neuroimage. 1996; 4:159–73. [PubMed: 9345506]
59. Scarr E, Dean B. Muscarinic receptors: do they have a role in the pathology and treatment of schizophrenia? J Neurochem. 2008; 107:1188–95. [PubMed: 18957051]
60. Minzenberg MJ, Firl AJ, Yoon JH, Gomes GC, Reinking C, Carter CS. Gamma Oscillatory Power is Impaired During Cognitive Control Independent of Medication Status in First-Episode Schizophrenia. Neuropsychopharmacology. Sep 8.2010 Epub ahead of print.
61. Sweet RA, Bergen SE, Sun Z, Marcsisin MJ, Sampson AR, Lewis DA. Anatomical evidence of impaired feedforward auditory processing in schizophrenia. Biol Psychiatry. 2007; 61:854–864. [PubMed: 17123477]
62. Spencer KM. The functional consequences of cortical circuit abnormalities on gamma oscillations in schizophrenia: insights from computational modeling. Front Hum Neurosci. 2009; 3:33. [PubMed: 19876408]

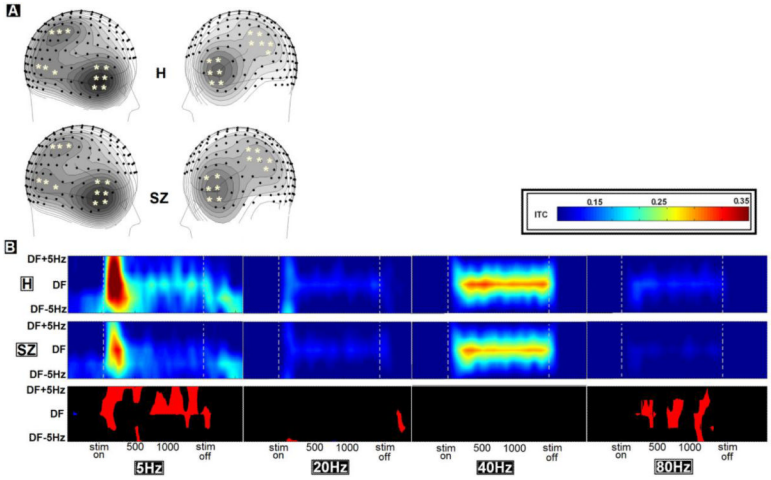

Figure 1.

A) Plots of inter-trial phase coherence (ITC) averaged across driving frequencies and stimulation interval time points, reveal similar distributions across MEG sensors for H (top) and SZ groups. B) ITC values (linearly interpolated from 2.5Hz resolution to .05Hz) from peak sensors (indicated with stars in A) averaged between hemispheres plotted across stimulation epochs for H (top) and SZ (middle) groups with periods of significant group differences (bottom) indicated as red (H>SZ) and blue (SZ>H). DF=driving frequency.

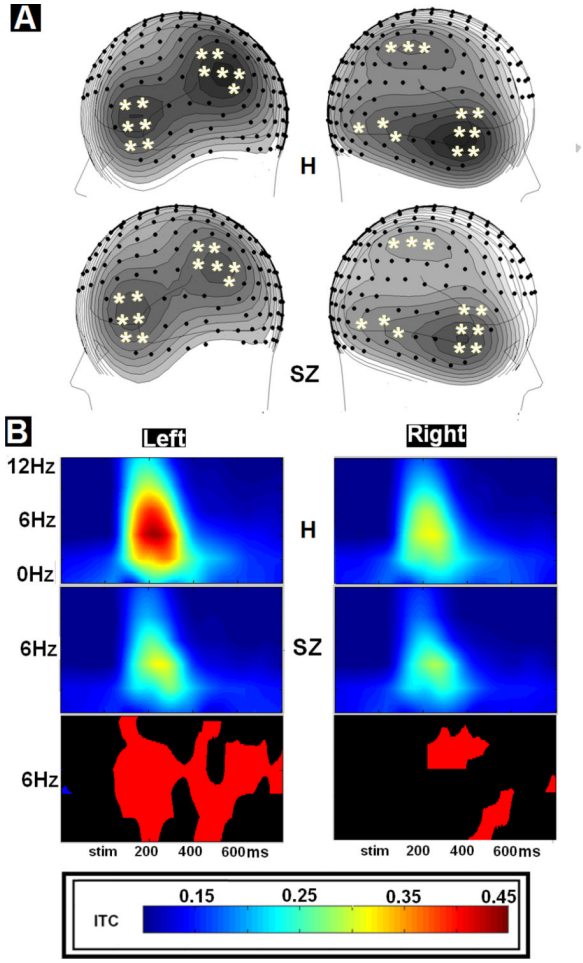

Figure 2.

A) Plots of inter-trial phase coherence (ITC) for 2.5–7.5Hz activity from 50–250ms, averaged across stimulus frequencies, reveal similar distributions across MEG sensors for H (top) and SZ groups. B) ITC values (linearly interpolated from 2.5Hz resolution to .25Hz) from peak sensors (indicated with stars in A) averaged across stimulus frequencies plotted for left and right hemispheres for H (top) and SZ (middle) groups with periods of significant group differences (bottom) indicated as red (H>SZ) and blue (SZ>H).

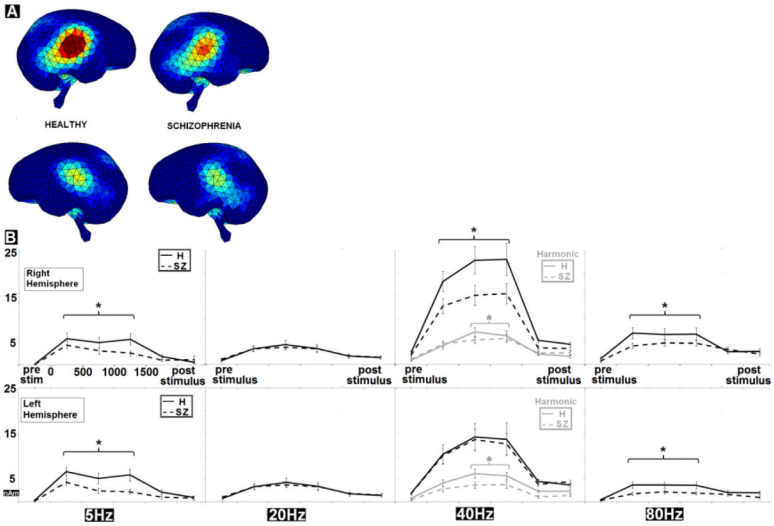

Figure 3.

A) Estimations of cortical source strength of activity averaged across steady-state driving frequencies and stimulation time bins and B) plotted across time bins and frequencies of stimulation for left and right hemisphere reveal bilateral differences to entrainment to stimulation in both hemispheres at 5-Hz and at 80-Hz, but only in right hemisphere at 40-Hz. Intervals marked with an * indicates significant group differences at $p<.05$ $F(1,32)$.

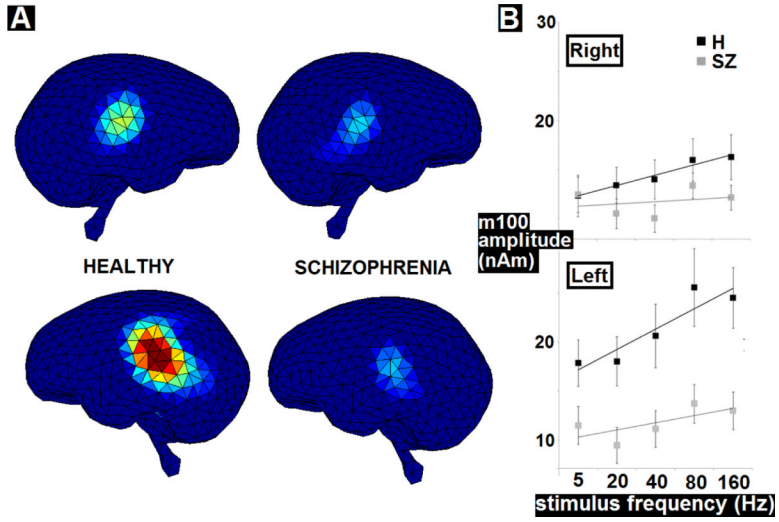

Figure 4.

A) Estimations of cortical source strength of M100 peaks averaged across stimulus frequencies and B) plotted across stimuli frequencies with fit lines calculated from group averages of slope and intercept. Error bars display standard error of the mean.

Table 1

Means presented with Standard deviations. Trials indices display number of useable trials for each condition. H, healthy control subjects; SZ, schizophrenia subjects; CPZ, chloropromazine; BPRS, Brief Psychiatric Rating Scale; SAPS, Scale for the Assessment of Positive Symptoms; SANS, Scale for the Assessment of Negative Symptoms.

	H	SZ	statistic	p-value
% female subjects	27.8	11.1	$\chi^2[1] = 1.59$	0.207
Age	**39.7** (21–56)	**40.7** (27–59)	t(35)=0.27	0.789
Medication dosage (CPZ equivalents)		**207.2** (0–400)		
BPRS (possible range: 24 to 168)	**28.05** (24–45)	**43.66** (29–61)	t(35)=5.53	<0.001
SANS (out of 102)		**32** (12–64)		
SAPS (out of 75)		**20** (0–52)		
Trials 5Hz	**88.00** (81–90)	**86.06** (68–90)	1.21	0.24
Trials 20Hz	**88.18** (80–90)	**88.12** (71–90)	0.04	0.97
Trials 40Hz	**86.23** (65–90)	**87.18** (72–90)	−0.49	0.63
Trials 80Hz	**387.76** (80–90)	**84.81** (65–90)	1.39	0.17
Trials 160Hz	**85.05** (65–90)	**82.13** (47–90)	0.94	0.31

Table 2

Rows display total percent variance explained, p-values for a two-tailed t-tests (n=32), and factor loadings for each variable. Columns display top 2 factors from Principal components analysis (PCA) with highest loadings highlighted.

	factor 1	factor 2
%variance	43.95	*23.86*
p-values (H vs SZ)	*0.003*	*0.012*
M100_slopes	0.76	−0.12
ITC M100 left	0.85	−0.06
aSSR 5Hz	0.66	0.16
ITC_aSSR_5Hz	0.90	0.03
aSSR 20Hz harm	−0.12	0.85
aSSR 4OHz R	−0.14	0.86
aSSR_80Hz	0.15	0.78
ITC aSSR 80Hz	0.15	0.70